INTERNATIONAL JOURNAL FOR NUMERICAL METHODS IN FLUIDS
Int. J. Numer. Meth. Fluids 2008; **56**:805–821
Published online 19 June 2007 in Wiley InterScience (www.interscience.wiley.com). DOI: 10.1002/fld.1550

Application of a second-order Runge–Kutta discontinuous Galerkin scheme for the shallow water equations with source terms

G. Kesserwani[1,2,*,†], R. Ghostine[1,2], J. Vazquez[1], A. Ghenaim[2] and R. Mosé[1]

[1]*U.P.R. Systèmes Hydrauliques Urbains, Ecole Nationale du Génie de l'Eau et de l'Environnement de Strasbourg, 1 quai Koch-BP 61039 F, 67070 Strasbourg Cedex, France*
[2]*Institut National des Sciences Appliqués, 24 boulevard de la Victoire, 67084 Strasbourg cedex, France*

SUMMARY

The present work addresses the numerical prediction of discontinuous shallow water flows by the application of a second-order Runge–Kutta discontinuous Galerkin scheme (RKDG2). The unsteady flow of water in a one-dimensional approach is described by the Saint Venant's model which incorporates source terms in practical applications. Therefore, the RKDG2 scheme is reformulated with a simple way to integrate source terms. Further, an adequate boundary conditions handling, by the theory of characteristics, was overviewed to be adapted to the external points of the mesh, as well as to some points of local invalidity of the Saint Venant's model. To validate the proposed technique, steady and transient test problems (all having a reference solution) were considered and computed by means of the overall method. The results were illustrated jointly with the reference solution and the results carried out by a traditional second-order finite volume (FV2) scheme implemented with the same techniques as the RKDG2. The proposed method has proven its practical consideration when solving discontinuous shallow water flow involving: non-prismatic channels, various cross-sections, smoothly varying bed topography and internal boundary conditions. Copyright © 2007 John Wiley & Sons, Ltd.

Received 28 November 2006; Revised 11 May 2007; Accepted 15 May 2007

KEY WORDS: 1D; boundary conditions; discontinuous flow; FV2; RKDG2; Saint Venant; source terms

1. INTRODUCTION

For many river flow applications, it is generally accepted that the unsteady flow of water in a one-dimensional approach is governed by the shallow water or the so-called Saint Venant equations. They represent the conservation of mass and momentum along the direction of the main flow. In conventional real-life applications, the inclusion of source terms is often necessary. Conversely,

*Correspondence to: G. Kesserwani, U.P.R. Systèmes Hydrauliques Urbains, Ecole Nationale du Génie de l'Eau et de l'Environnement de Strasbourg, 1 quai Koch-BP 61039 F, 67070 Strasbourg Cedex, France.
†E-mail: georges.kesserwani@engees.u-strasbg.fr

the presence of extreme slopes, high roughness and changes of the waterway geometry represents a difficulty that can lead to numerical inaccuracies arising from the source terms of the equations.

It has traditionally been difficult to have only one method able to reproduce automatically any general solution. Several high-resolution Godunov-type methods [1, 2] have been developed to solve the shallow water equations with source terms demonstrating the accuracy, effectiveness and robustness of such methods. Bermudez and Vázquez [3] proposed an upwind method for shallow water equations with bed slope source term and Vázquez-Cendón [4] applied the same idea to solve more shallow water flow problems. Recently, Hubbard and García-Navarro [5] proposed a scheme by balancing source terms and flux gradients, in which the upwind method of Bermudez and Vázquez [3] is used for source terms. Zhou *et al.* [6] pioneered the application of the surface gradient method for the treatment of the source terms. This technique can be used in any high-resolution Godunov-type scheme which requires data reconstruction. The authors' framework has been successfully applied to simulate the shallow water equations with bed slope source terms.

Over the last few years, literature has dealt considerably with Runge–Kutta (RK) discontinuous Galerkin (DG) schemes [7–10]. This class of finite element methods has seen a very significant attention and has proven its aptness in solving hyperbolic conservation laws. The key feature of the RKDG method is that it invokes finite volume tools such as: the exact or approximate Riemann solver to evaluate flux at interfaces [2, 11], total variation diminishing (TVD) RK time stepping [12], and slope limiters [13–15] to avoid spurious oscillation in the vicinity of strong shocks. A RKDG method has the advantage of flexibility in handling complex geometries, *hp*-adaptivity, and efficiency of parallel implementation and has been used successfully in many applications [10]. For more information about the recent development of the DG method, we refer the reader to the recent special issues established by Cockburn and co-workers [7, 9].

It is only recently that the DG method has been applied to shallow water equations. Schwanenberg and Kongeter [10] presented the first implementation of the RKDG method for shallow water equations and its application to practical problems. The authors developed a local DG method for shallow water model where they used the Harten and Lax numerical flux [16]. The method has been applied to simulate flows involving shocks, such as dam-break flows and oblique hydraulic jumps. Most recently, Xing and Shu [17] have extended the high-order finite volume WENO and finite element DG schemes to solve a class of conservation laws with separable source terms—particularly applications to the shallow water equations were examined.

The main intention of this survey is to inspect the performance of a second-order RKDG (RKDG2) scheme. We aim at computing, by means of the RKDG2 method, discontinuous flow problems (transcritical flow with shocks, hydraulic jumps) involving source terms (slowly varying bed topography, channel breadth variation, rectangular and trapezoidal cross-sections). Hence, the RKDG2 scheme is rewritten and detailed in an explicit form as a means to simulate the shallow water equations. The algorithms were implemented in conjunction with Roe's Riemann solver [11] and a simple pointwise treatment of the source terms. Moreover, an explanation of the boundary conditions handling, by the theory of characteristics [18], is briefly reported. Finally, a set of various steady and transient flow problems [1, 5, 18–21], all having a reference solutions, has been selected and computed exemplifying the performance of the traditional RKDG2 scheme *versus* the performance of a traditional FV2 method [2]. Both of the finite element and the finite volume solvers were implemented using the same: source terms treatment; Riemann solver [11]; slope limiter function [14]; and boundary conditions management [18].

The lay out of this paper is as follows. In Section 2, we present the governing equations. Section 3 presents an explicit formulation of the proposed RKDG2 scheme. Section 4 describes

DOI: 10.1002/fld

the treatment of the boundary conditions. Section 5 is devoted for the numerical tests and results.

2. GOVERNING EQUATIONS

Recent schemes are based on the conservative formulation of the Saint Venant equations, because it is related closely to the fluxes action on the flow

$$U_t + F_x = G \quad \text{in } [0, L] \times [0, T] \tag{1}$$

where

$$U = \begin{pmatrix} A \\ Q \end{pmatrix}, \quad F = \begin{pmatrix} A \\ Q^2/A + gI_1 \end{pmatrix} \quad \text{and} \quad G = \begin{pmatrix} 0 \\ gA(S_0 - S_f) + gI_2 \end{pmatrix}$$

t represents time in s, x the longitudinal distance in m, U is the conserved variable or the flow vector, F the flux vector and G is the source terms vector. A is the wetted cross-sectional area in m^2, Q the flow discharge in m^3/s, g the acceleration due to gravity in m/s^2. $S_0 = -\partial z/\partial x$ is the bed slope where $z(x)$ represents the bed elevation in m. S_f represents the friction slope defined in terms of the Manning's roughness coefficient n_m [22]. I_1 and I_2 are, respectively, the hydrostatic pressure and wall pressure terms. They can be evaluated from

$$I_1 = \int_0^{h(x)} [h(x) - \eta]\sigma(x, \eta)\, d\eta \quad \text{and} \quad I_2 = \int_0^{h(x)} [h(x) - \eta](\partial\sigma/\partial x)_{h=h_0}\, d\eta \tag{2}$$

where h is the level of the free surface in m, η is the depth integration variable and σ corresponds to the channel width at a particular depth. For a rectangular cross-section, $I_1 = A^2/(2b)$ and $I_2 = b'A^2/(2b^2)$, where $b(x)$ is the width of the channel's bottom in m.

Using the jacobian matrix ($J = \partial F/\partial U$) of the flux vector with respect to the flow vector, Equation (1) can be expressed in a quasi-linear form:

$$U_t + JU_x = G \tag{3}$$

J has two real eigenvalues $a^{1,2} = u \pm c$, where $u = Q/A$ is the mean velocity and $c = \sqrt{gA/B}$ is the wave celerity (B is the channel width at the free surface). The hyperbolic nature of the equation ensures that matrix J has a complete set of independent and real eigenvectors $e^{1,2} = (1, a^{1,2})^t$.

For a non-prismatic rectangular channel, the total derivative of the flux vector dF/dx involves, in addition to the partial derivative with respect to the conserved variable (JU_x), a partial derivative with respect to the width variation $(\partial F/\partial b) \times b'(x)$. Following the work of García-Navarro and Vázquez-Cendón [23], the supplementary partial derivative has been moved to the RHS of Equation (3). And consequently, the source terms vector is modified to $G' = G - (\partial F/\partial b) \times b'(x)$.

3. RKDG2 SCHEME

In the following section, the governing equations are discretized. The computational domain $[0, L]$ is divided into N uniform cells $I_i = [x_{i-1/2}, x_{i+1/2}]$ where the points x_i are the centres of the cells,

DOI: 10.1002/fld

and $\Delta x = x_{i+1/2} - x_{i-1/2}$ the cell's size, assumed to be uniform. In this survey, the RKDG method is considered according to the approach of Cockburn and Shu [8]. We seek a local approximation U_h to U such that for each time $t \in [0, T]$, U_h belongs to the finite dimensional space $P^k(I_i)$ of polynomial in I_i of degree at most k. Therefore, system (1) is multiplied by a continuous test function v_h and integrated over I_i. Afterward, the flux term is integrated by part to obtain the following weak formulation:

$$\int_{I_i} \partial_t U_h v_h \, \mathrm{d}x - \int_{I_i} F(U_h) \partial_x v_h \, \mathrm{d}x + [F(U_h) v_h]_{i+1/2} - [F(U_h) v_h]_{i-1/2} = \int_{I_i} G(U_h) v_h \, \mathrm{d}x \quad (4)$$

The key feature of the DG method is that the solutions are allowed to be discontinuous over elemental boundaries. Thus, the function U_h is discontinuous at points $x_{i+1/2}$. Therefore, the physical flux function F has to be replaced by a numerical flux function, depending on the two different values of U_h at the points $x_{i+1/2}$ as it will be discussed later.

In the aim of decoupling the system, we adopt the Legender polynomials (P_m) as local basis functions to obtain a diagonal mass matrix. As in the standard DG we chose $\varphi_m^i(x) = P_m(2(x - x_i)/\Delta x)$ as a test function v_h. In this paper, the interest will be constrained to a second-order space accuracy scheme, thus the method was set up for $k = 1$, corresponding to piecewise linear approximations. Therefore, two basis functions $\{\varphi_0^i(x), \varphi_1^i(x)\}$ are needed and the approximation of the solution $U_h(x, t)$ over each cell I_i can be written as follows:

$$U_h(x, t)|_{I_i} = U_i^0(t) + 2U_i^1(t)(x - x_i)/\Delta x \quad \forall x \in I_i \quad (5)$$

Consequently, at each time step, we have to solve for $\{U^0(t), U^1(t)\}$ going from the projected initial condition, which will be defined by the following degrees of freedom:

$$U_i^m(0) = (2m + 1)/\Delta x \int_{I_i} U(x, 0) \varphi_m^i(x) \, \mathrm{d}x, \quad m = 0, 1 \quad (6)$$

In the treatment of the integral terms of Equations (4) and (6) we used quadrature rules. Here $k = 1$ is the earlier mentioned order of the approximating polynomial. For Gaussian rules, one requires $(k + 1)$ nodes to conserve the accuracy order of the full method. This means that for $m = 0, 1$ it suffices to use an $(m + 1)$ points Gaussian quadrature rules, respectively. Then the initial condition will have the following form:

$$U_i^0(0) = U(x_i, 0) = U_0(x_i) \quad \text{and} \quad U_i^1(0) = \sqrt{3}/2[U_0(x_i + \Delta x\sqrt{3}/6) - U_0(x_i - \Delta x\sqrt{3}/6)]$$

To determine the approximate solution, at each time step, we have to find the evolution of the degrees of freedom as follows:

$$\mathrm{d}U_i^m/\mathrm{d}t = L_m(U^0, U^1) \quad \text{for } m = 0, 1 \quad (7)$$

L_0 and L_1 are the DG space operators. After the integrals approximation and by the use of the Legender polynomials properties, these operators will have the following form:

$$L_0(U^0, U^1) = -1/\Delta x[\tilde{F}(\hat{U}_{i+1/2}^+, \hat{U}_{i+1/2}^-) - \tilde{F}(\hat{U}_{i-1/2}^+, \hat{U}_{i-1/2}^-) - \Delta x G(U_i^0)] \quad (8)$$

$$L_1(U^0, U^1) = -3/\Delta x[\tilde{F}(\hat{U}_{i+1/2}^+, \hat{U}_{i+1/2}^-) + \tilde{F}(\hat{U}_{i-1/2}^+, \hat{U}_{i-1/2}^-) - F(U_i^0 - U_i^1/\sqrt{3}) - F(U_i^0 + U_i^1/\sqrt{3}) - \Delta x\sqrt{3}/6(G(U_i^0 + U_i^1/\sqrt{3}) - G(U_i^0 - U_i^1/\sqrt{3}))] \quad (9)$$

DOI: 10.1002/fld

where $U^{\pm}_{i+1/2} = U_h(x^{\pm}_{i+1/2}, t)$ are the left and right limits of the discontinuous solution U_h at the cell's interface. To maintain the stability and the non-oscillatory property of the RKDG2 method in the presence of strong shocks, $U^{\pm}_{i+1/2}$ were replaced by the borders ($\hat{U}^{\pm}_{i\pm1/2}$) of the slope limited solutions where the classical *minmod* [14] function was applied according to the Osher's slopes definition [13]. They are given by

$$\hat{U}^{\mp}_{i\pm1/2} = U^0_i \pm minmod(U^1_i, U^0_i - U^0_{i-1}, U^0_{i+1} - U^0_i) \tag{10}$$

$\tilde{F}(U^-, U^+)$ is the numerical flux function based on the approximate Riemann solver of Roe [11]. Its expression takes the following form:

$$\tilde{F}(U^-, U^+) = 0.5\left[F(U^-) + F(U^+) - \sum_{p=1}^{2} \alpha^p_{\text{int}} |\tilde{a}^p_{\text{int}}| \tilde{e}^p_{\text{int}}\right] \tag{11}$$

where, the subscript 'int' designates the intermediate state between the left and right states. Once the Roe average velocity and celerity ($\tilde{u}_{\text{int}}, \tilde{c}_{\text{int}}$) are found, the mean eigenvalues $\tilde{a}^p_{\text{int}}$ and eigenvector $\tilde{e}^p_{\text{int}}$ are found. An average of pth waves strength α^p_{int} is found by an explicit formula involving $U^-, U^+, \tilde{u}_{\text{int}}$ and $\tilde{c}_{\text{int}}$ [23].

A well-known problem that occurs when using the Roe's Riemann solver is the possibility of having unphysical expansion shocks in the solution [2]. Instead of the required fan, a discontinuous shock is chosen by the Riemann solver to represent the expansion. Hence, the absolute eigenvalues are modified using an entropy fix, namely:

$$|\tilde{a}^p_{\text{int}}|^* = \begin{cases} |\tilde{a}^p_{\text{int}}| & \text{if } |\tilde{a}^p_{\text{int}}| \geqslant \varepsilon^p \text{ where} \\ (\tilde{a}^p_{\text{int}})^2/(2\varepsilon^p) + \varepsilon^p/2 & \text{if } |\tilde{a}^p_{\text{int}}| < \varepsilon^p \ \ \varepsilon^p = \min[\tilde{c}_{\text{int}}, \max(0, 2((a^p)^+ - (a^p)^-))] \end{cases}$$

The second space order semi-discrete scheme, (8) and (9), is discretized in time by a nonlinearly stable two step RK mechanism [12] leading to a second-order accuracy scheme in time and space. Thus, the time stepping for each degree of freedom is:

$$\begin{aligned} (U^{0,1})^{\text{int}} &= (U^{0,1})^n + \Delta t L_{0,1}((U^0)^n, (U^1)^n) \\ (U^{0,1})^{n+1} &= 0.5[(U^{0,1})^n + (U^{0,1})^{\text{int}} + \Delta t L_{0,1}((U^0)^{\text{int}}, (U^1)^{\text{int}})] \end{aligned} \tag{12}$$

According to the stability analysis (performed for scalar non-linear hyperbolic conservation laws) of Cockburn and Shu [8], the choice of the CFL [24] number depends on the desired order of accuracy of the scheme and was chosen equal to 0.333. Hence, the time step is calculated:

$$\Delta t = \text{CFL}\Delta x / \min_i (|u| + c)^n_i \tag{13}$$

For a better comprehension of the approximating polynomials' structure, we illustrate in Figure 1 the numerical evolution of the piecewise linear approximations after 61 time step going from a constant initial condition. This simulated problem will be discussed later. However, in order to adjudicate with respect to a reference solution and a finite volume scheme, only mean values of the polynomial approximations will be considered in the figure plots of Section 5.

DOI: 10.1002/fld

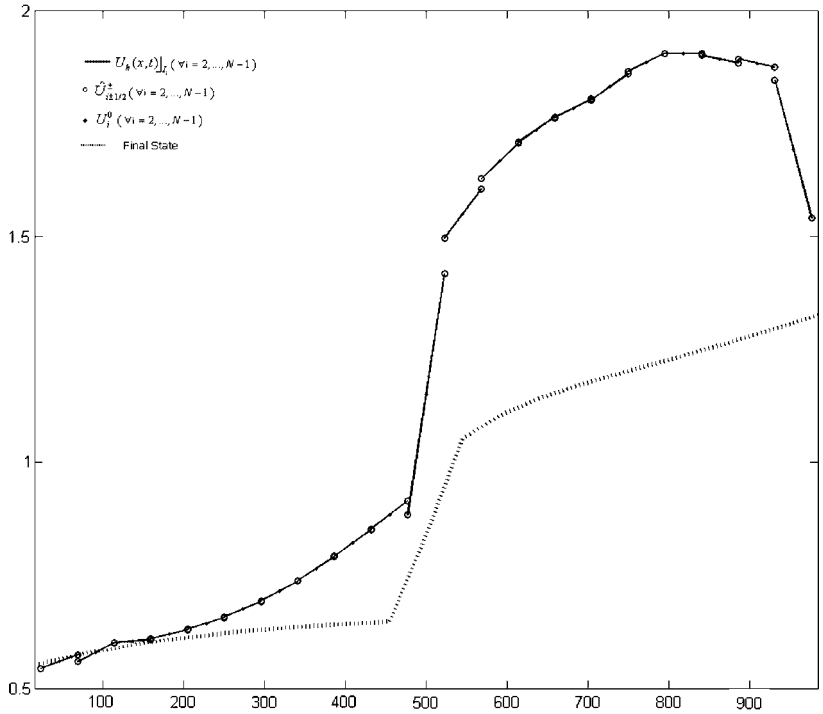

Figure 1. Evolution of the approximating polynomials after 61 time steps.

4. BOUNDARY CONDITIONS

Although the characteristic form of the Saint Venant's momentum equation has lost almost all reference to the forces and fluxes included for the conservation of momentum, this form provides insight into shallow-water wave motion, which is not evident in the other forms. This form is a transformation of Saint Venant's momentum equation where the derivatives are taken in the proper directions, called characteristics directions, and can be written as ordinary derivatives and not partial derivatives. The Saint Venant characteristic form is

$$(\partial Q/\partial t + (u \pm c)\partial Q/\partial x) + (-u \pm c)(\partial A/\partial t + (u \pm c)\partial A/\partial x) = gA(S_0 - S_f) + gI_2 \qquad (14)$$

where the above differential operators ($d^{\pm}/dt = \partial/\partial t + (u \pm c)\partial/\partial t$) are in fact the total derivatives along the characteristic lines defined by $dx/dt = u \pm c$ (denoted by $C+$ and $C-$).

In practical applications, every channel is of finite length; at some point the analysis starts and at another it ends, so boundaries must be defined. Possible conditions at the boundaries of a channel are shown in Figure 2. If the flow is subcritical, the interval of dependence [2] for the upstream most point on the channel is somewhat upstream from the boundary point. Thus, estimation of flow conditions at this boundary point requires information about the flow conditions upstream of the boundary. The ($C+$) trajectory from upstream points affects the flow at that point in the (x–t) plan; therefore, a single condition must be specified at the boundary point. This kind of boundary conditions can be called physical boundary conditions. As the ($C-$) curve leaves the

DOI: 10.1002/fld

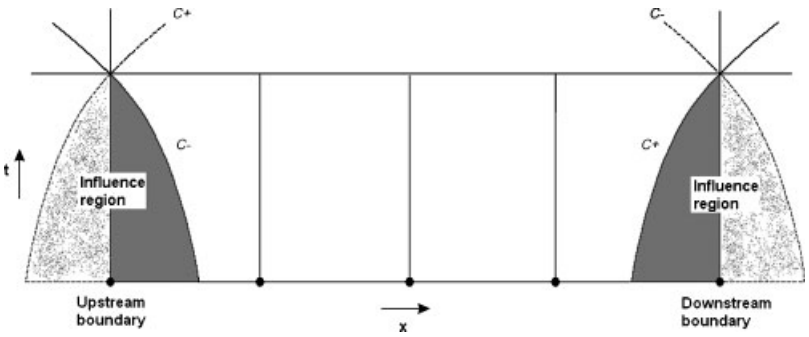

Figure 2. Characteristic curves at boundary points for subcritical flow.

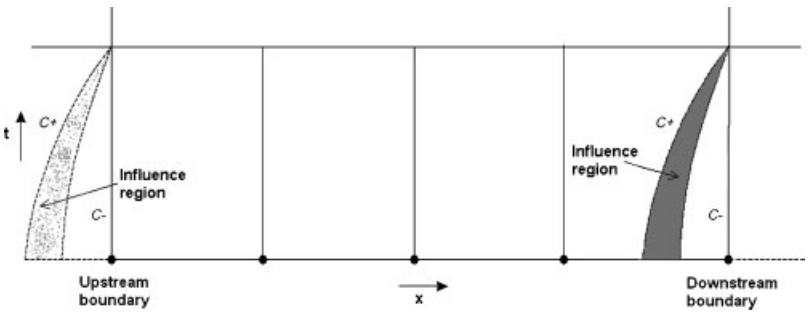

Figure 3. Characteristic curves at boundary points for supercritical flow.

domain, the influence region belongs to the computational domain and the information linked to that characteristic curve depends exclusively on interior points. These kinds of boundary conditions are called numerical boundary conditions. Again, at the downstream boundary, part of the interval of dependence falls outside the channel length being analysed, and a physical downstream-boundary condition must be supplied. The numerical boundary condition is to be integrated from the Saint Venant characteristic form along the $(C+)$ characteristic curve. If the flow is supercritical at a boundary, the required number of conditions changes. At an upstream boundary, the flow and the elevation of water must both be supplied because, as shown in Figure 3, the interval of dependence of points on the upstream boundary in the $(x–t)$ plan are outside the length of channel analysed. At the downstream end, no boundary conditions are required because the interval of dependence falls within the length of channel analysed. Therefore, both of the $(C+)$ and $(C-)$ characteristic curves should propagate information from upstream to downstream. Imposing any values in this case would over specify the problem and represent a contradiction to the mathematical theory. In this situation, two numerical boundary conditions are calculated by differentiating the Saint Venant characteristics form along both $(C+)$ and $(C-)$ curves.

The most usual physical boundary conditions at the inlet are a discharge hygrograph $Q(t)$ or a water depth limnigraph $h(t)$ in case of subcritical flow and both together in case of supercritical flow. In finding numerical boundary conditions we followed the framework of García-Navarro

DOI: 10.1002/fld

and Savirón [18], who gave the insight on how to apply the theory of characteristics to deal with numerical boundary conditions of open channel flow problems with the McCormack's method.

5. NUMERICAL TESTS AND RESULTS

In this section the proposed implementation of the RKDG2 scheme is verified by solving some relevant benchmark problems presented in the literature [1, 5, 18–21]. The classical idealized dam-break problem, used in several papers to evaluate shock-capturing schemes is examined first. Subsequently, steady discontinuous flow problems involving source terms (friction terms; bed and/or width variation; rectangular and trapezoidal cross-sections) are investigated. Therefore, the unsteady model is given steady boundary conditions, and the limiting steady solution is compared with an available reference solution. Moreover, a flow problem involving internal boundary conditions was broached so as to ensure that: the RKDG2 scheme is able to deal with flows over compound branches coupled with internal boundary conditions.

To achieve a better interpretation, we will exhibit the RKDG2 scheme's results close to the results of a traditional FV2 method. This scheme is broadly known as the TVD Lax-Wendroff [2] and is, as well, second-order accurate in space and time; its numerical flux function consists of the Roe's first-order flux coupled with a flux limited second-order term. It is worth noting that the latter scheme was, as well, implemented along with the *minmod* slope limiter [14] and the pointwise treatment the source vector. For the convergence (stopping) criteria in the simulation of the steady problems, we used the L^2 norm where subsequent iteration results were compared. These varieties of numerical results demonstrate the ability of the RKDG2 method to produce generically more accurate solutions than the FV2 scheme.

5.1. Transient idealized dam-break problem

We considered a dam, in a wide ($b = 10$ m) frictionless channel with a flat-bottom surface, initially located at the middle of the 2000 m long rectangular channel. A discontinuous initial condition defines the non-linear problem, and we have studied the evolution of the free surface and the flow discharge after 50 s of the dam breaking. This initial conditions led to a shock-wave propagation to the downstream and a rarefaction wave propagation to the upstream. Two cases were set according to the initial depth ratio h_u/h_d, where h_u and h_d denote, respectively, the water depths upstream and downstream of the dam. The first case corresponds to a depth ratio of 4 (Figure 4) and the second to a ratio of 20 (Figure 6). Since the flow during 50 s did not reach boundaries; we applied, exclusively for this test problem, transitive boundary conditions for the upstream and downstream borders. In the simulation, the space interval of the mesh is $\Delta x = 20$ m and the first case's results are illustrated in Figure 5 along with the FV2 scheme's results and the analytical solution [19]. The second case's results are displayed in Figure 7, where good captures of the discontinuities evolution were achieved by the advised scheme. However, it is worth noting that the corresponding governing equations of this problem are characterized by a zero source vector ($G = 0$). Then, more realistic problems are investigated below, where source terms components ($G \neq 0$) must be incorporated.

5.2. Steady hydraulic jump in a prismatic rectangular channel

The channel's bed, the free surface and critical levels of this problem are illustrated in Figure 8. It is a steady problem of a hydraulic jump modelling in a 1000 m long rectangular prismatic

DOI: 10.1002/fld

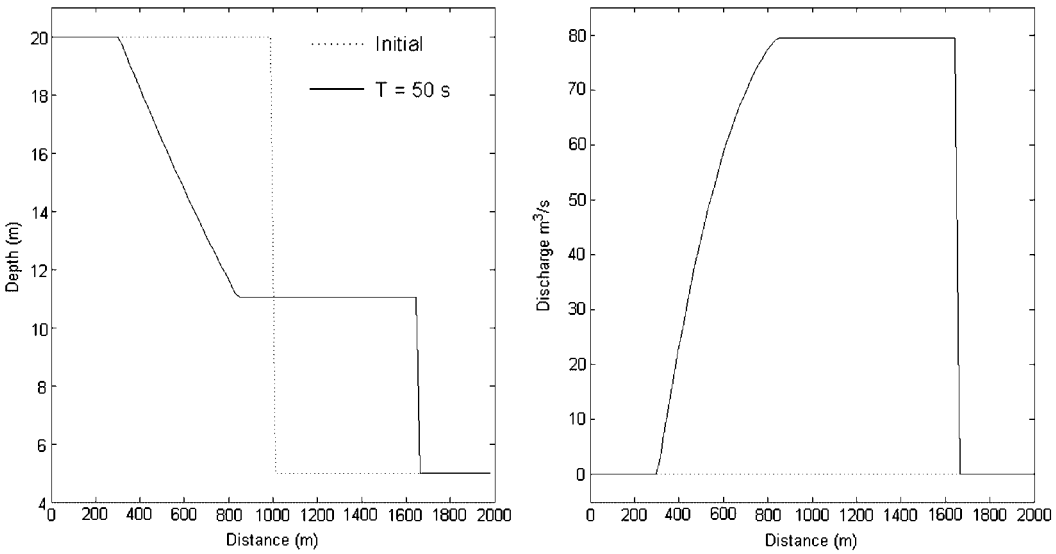

Figure 4. Initial condition and exact solution for the unsteady dam-break problem; $h_u/h_d = 4$.

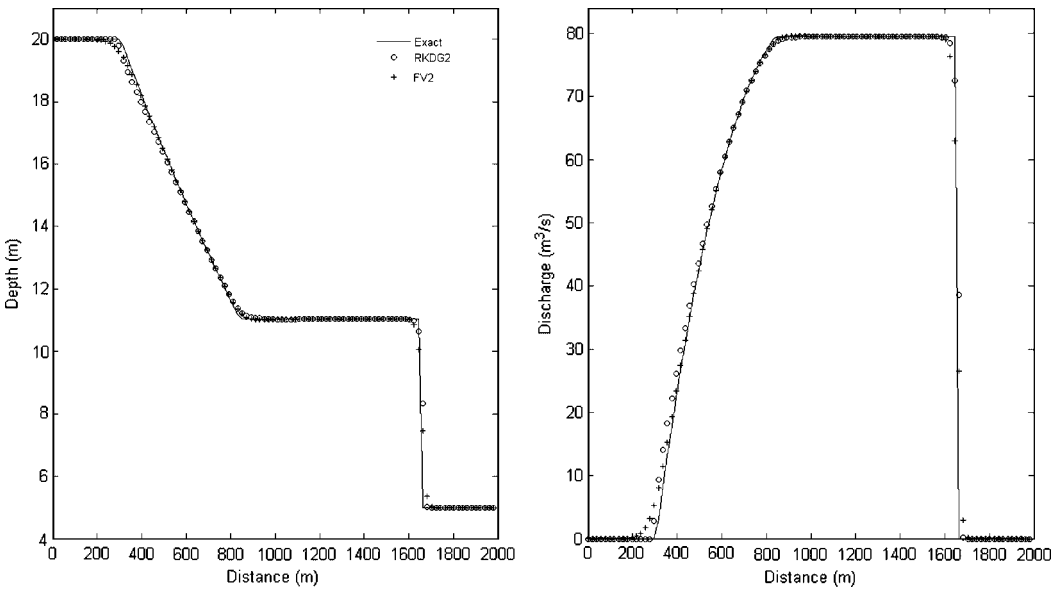

Figure 5. Flow variables' plots simulated by RKDG2 and FV2.

channel of width $b = 10\,\text{m}$ with a Manning's roughness coefficient of $n_m = 0.02$ and a spatially varying bed slope. The inflow discharge is $Q = 20\,\text{m}^3/\text{s}$. The flow, supercritical at the upstream, changes *via* a hydraulic jump to be subcritical halfway along the channel, and remains subcritical thereafter. Therefore, the water depth ($h_u = 0.543853\,\text{m}$) and the water discharge $Q = 20\,\text{m}^3/\text{s}$

DOI: 10.1002/fld

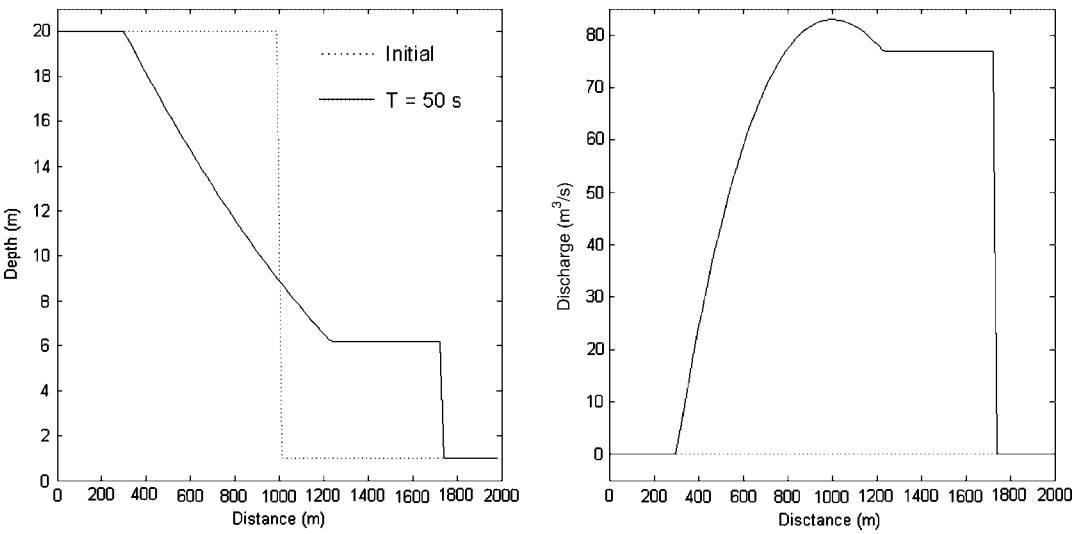

Figure 6. Initial condition and exact solution for the unsteady dam-break problem; $h_u/h_d = 20$.

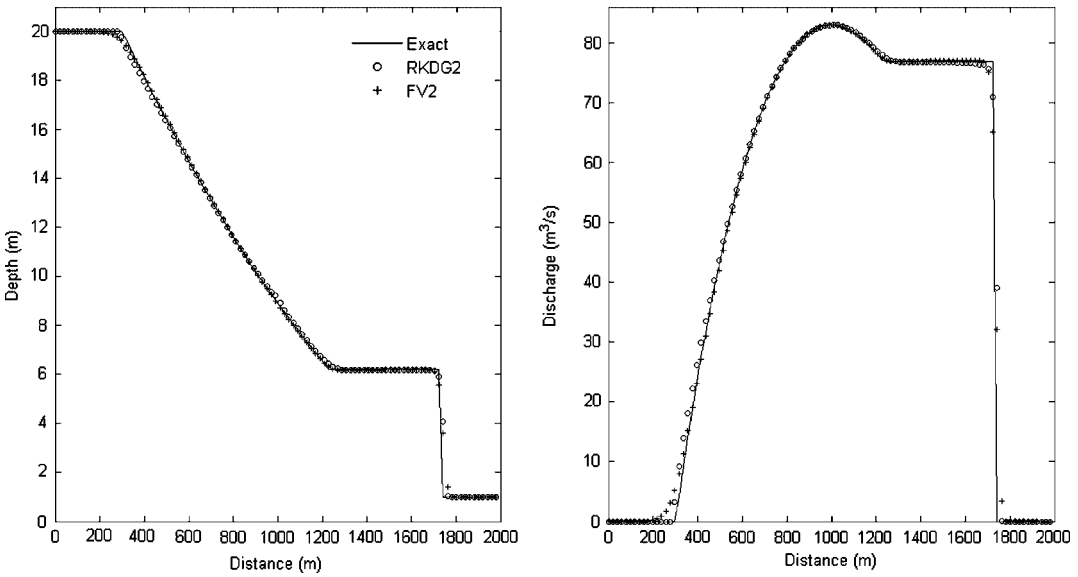

Figure 7. Depth and discharge computed by RKDG2 and FV2.

must be specified for the upstream boundary condition. At the downstream end, we specify only one physical condition ($h_d = 1.334899$ m) as the flow is subcritical, and for the water discharge we proceed by a numerical boundary condition. For the derivation of the analytical solution and the bed slope see McDonald *et al.* [21]. In the simulation, the space interval of the mesh is $\Delta x = 25$ m. The resolutions of the finite element and the finite volume solver are displayed in

DOI: 10.1002/fld

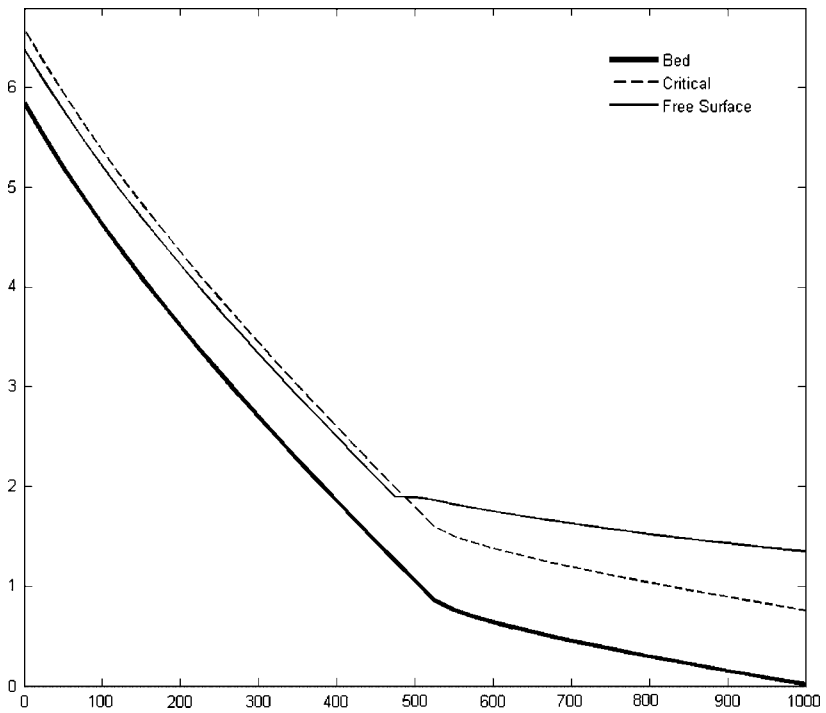

Figure 8. Flow properties of the hydraulic jump problem listed in Section 5.2.

Figure 9, both against the exact solution. The RKGD2 scheme and the FV2 scheme appear to have fair similar outcomes for the water stage profile. A poor maintenance of the steady-state discharge was achieved by the FV2 scheme which is not present in the RKDG2 results, notably after the discharge peak.

5.3. Transcritical flow, with shock, over a hump in a non-prismatic channel

It is about a steady water flow over a hump in a converging–diverging conduit. This channel is 3 m long with a smoothly varying bed and width giving the channel a symmetrical form (Figure 10). Again the flow regime is dependent on the boundary conditions. Our test case here is that of a transcritical flow with a stationary shock downstream of the hump and a critical point at the throat. The flow, subcritical at the upstream, turns to supercritical at the middle of the channel and then returns to subcritical at the downstream passing through a shock. Following Reference [5], the initial condition is $h+z=1$ m and $Q=1.8796\,\mathrm{m}^3/\mathrm{s}$. Since the flow regime is subcritical at the inflow and the outflow, one boundary condition should be specified at the upstream and at the downstream. For the upstream boundary condition we require the water discharge ($Q=1.8796\,\mathrm{m}^3/\mathrm{s}$) and the water depth is found by a numerical boundary condition. For the downstream boundary, a water depth of $h_\mathrm{d}=1$ m is imposed as a physical boundary condition and the water discharge is set up by a numerical boundary condition. An analytical solution can be calculated for each point in the channel by solving a cubic equation that derives from conservation of water energy. The space interval of the mesh is $\Delta x=0.0375$ m. Figure 11 is a plot of the results provided by the two

DOI: 10.1002/fld

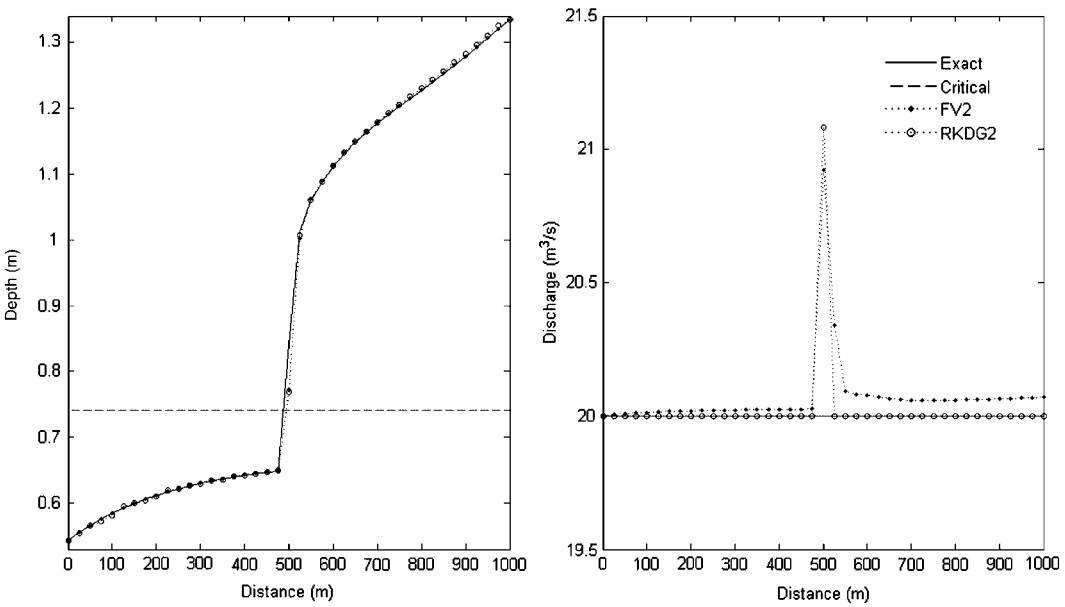

Figure 9. Hydraulic jump and discharge profiles computed with RKDG2 and FV2.

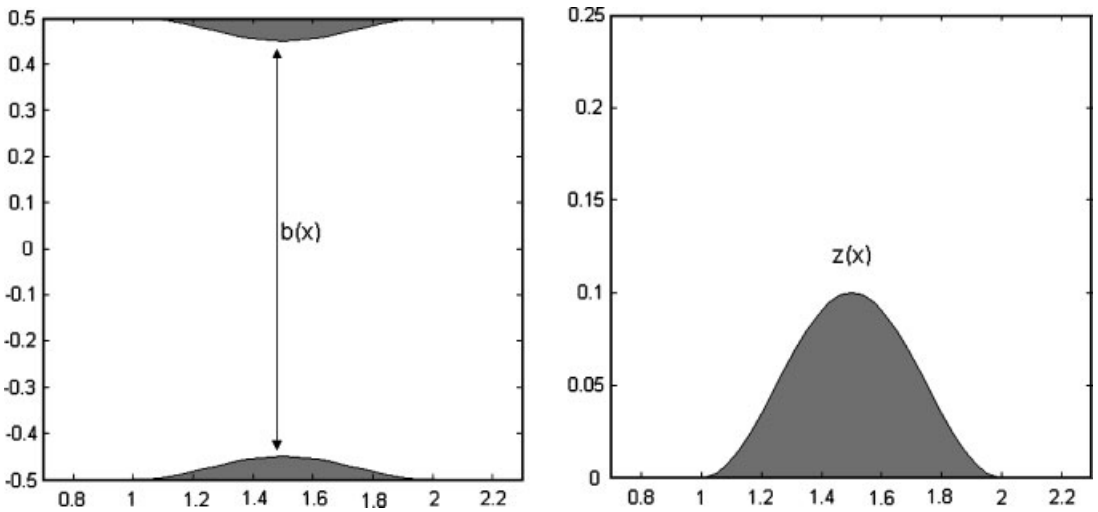

Figure 10. Bed and width geometry of the conduit detailed in the Section 5.3.

schemes. The depths and the discharges profiles, carried out by both RKDG2 and FV2 schemes, are in a good agreement with the exact solution. However, a good resolution of the trailing discontinuity was accomplished by RKDG2.

DOI: 10.1002/fld

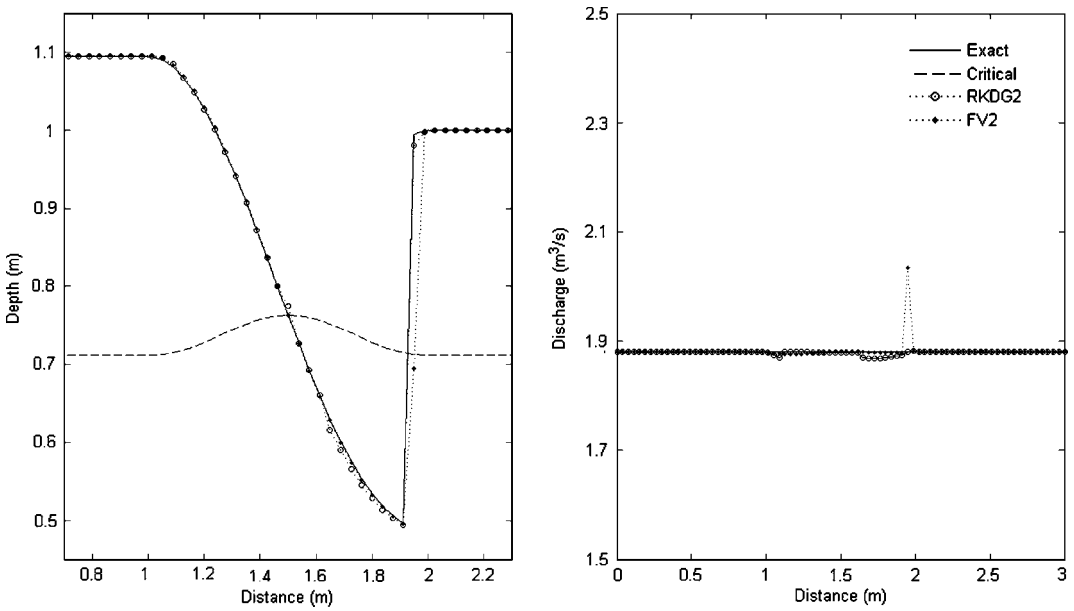

Figure 11. Display of the flow variables simulated by RKDG2 and FV2.

5.4. A succession of transcritical flows with shocks in a trapezoidal conduit

This example is taken from Reference [21], where a series of cases with analytical solutions are generated for problems with non-flat beds. This hydraulic problem consists of a 650 m long trapezoidal channel with a bed variation given by a slope function of x and a roughness coefficient $n_{\mathrm{m}} = 0.03$. For more understanding of this flow problem, we show in Figure 12 the bed slope variation and the flow properties according to the bed level and critical level. The flow is enforced to be supercritical at the upstream and the downstream. Consequently, two physical boundary conditions were specified at the upstream ($Q = 20\,\mathrm{m}^3/\mathrm{s}$ and $h_{\mathrm{u}} = 0.850\,\mathrm{m}$). At the downstream, two numerical boundary conditions were calculated as discussed in the previous section. This example is characterized by a fast variation in the flow regime from supercritical to subcritical generating a succession of stationary shocks and points of transcritical flow. The space interval of the mesh is $\Delta x = 8.125\,\mathrm{m}$. Figure 13 contains the discharge and water depth plots. The numerical results achieved by the RKDG2 scheme proved more advantageous. As in the hydraulic jump problem (5.2); although FV2 gives a very close approximation to the stage model carried out by RKDG2, it was very poor at predicting the flow discharge where discrepancies in the solutions have occurred. On the contrary, these regions (between the discharge peaks) were well matched by RKDG2.

5.5. Steady flow over a ladder of weirs

In open channel flow simulation, some points of local inapplicability for the Saint Venant channel flow equations may exist. One typical example is the flow over weirs. The whole model may be considered as a set of reaches computed with the Saint Venant equations and linked by special points where different laws are introduced. This test example [1] involves the computation of a

DOI: 10.1002/fld

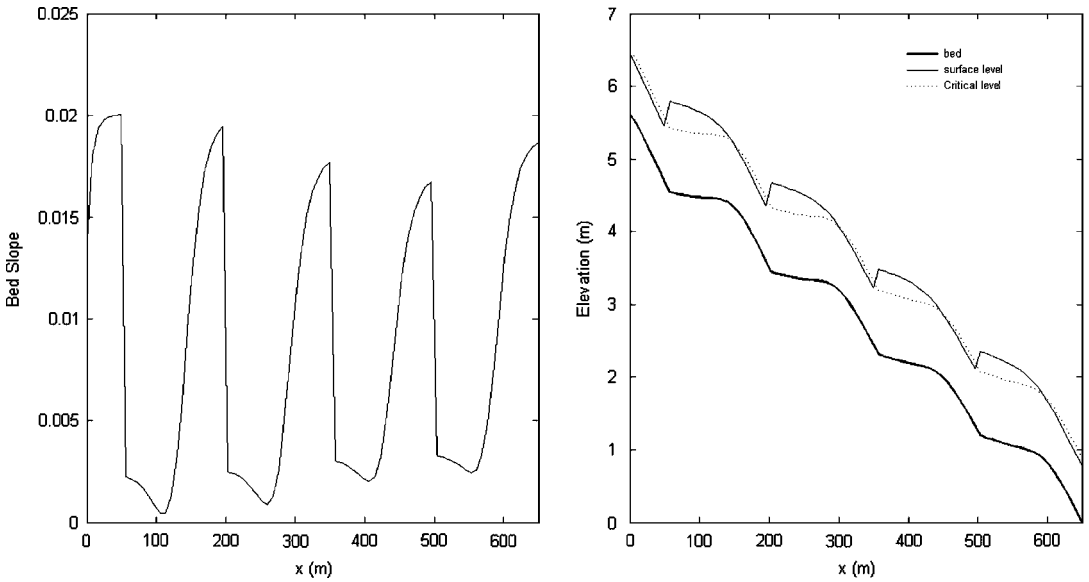

Figure 12. Slope variation and flow properties for the problem detailed in Section 5.4.

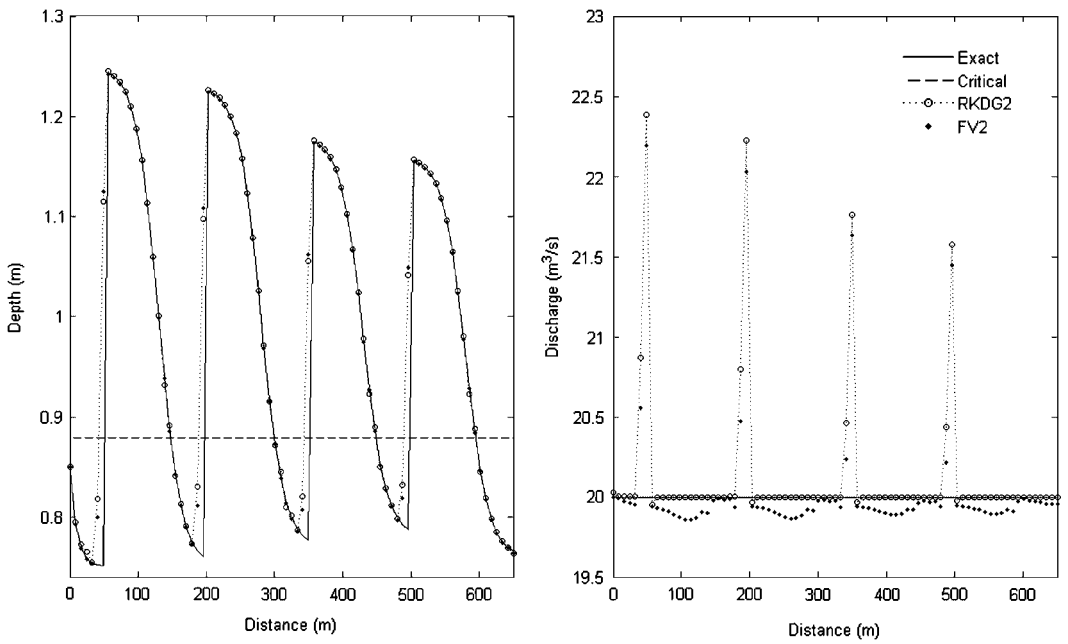

Figure 13. Water depth and flow discharge computed by RKDG2 scheme and FV2.

discontinuous stationary flow in a 500 m long rectangular channel, 6 m wide that contained three identical weirs of 0.25 m in height. The bottom slope was $S_0 = 0.008$, and the Manning's roughness coefficient was $n_m = 0.015$. The discharge was $20\,m^3/s$, and the initial water depth was set 2 m.

DOI: 10.1002/fld

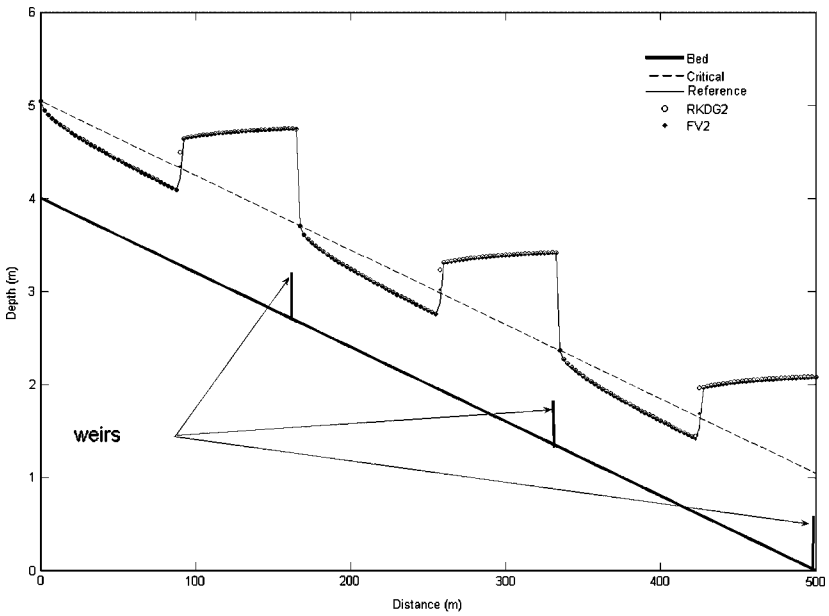

Figure 14. Free surface profile over a ladder of weirs computed by RKDG2 and FV2.

For the flow over the internal weirs, a numerical boundary condition coupled with the weir equation was performed for the approximate solution corresponding to the cell preceding each internal weir. While, for the approximate solution relative to the cell following each weir we adopt a numerical boundary condition coupled with a discharge conservation condition.

In treatment of external boundaries, one physical condition is imposed at the upstream ($Q = 20\,\mathrm{m}^3/\mathrm{s}$) and a numerical boundary condition is calculated. At the downstream, a numerical boundary condition coupled with the weir equation was set. The weir relation used for the boundary conditions treatment is: $u = 2/3 \times C_\mathrm{d} \times \sqrt{2g} H_\mathrm{w}^{3/2}$, where $C_\mathrm{d} = 1.39$ is the coefficient of the discharge and H_w is the water depth above the level of the weir.

The results achieved by FV2 and RKDG2 are illustrated in Figure 14 and found to compare favorably with a reference solution. This reference solution was obtained by applying the first-order upwind scheme of Roe [11] implemented with the upwind treatment of the source terms [3]. It is worth stressing that this latter scheme produces second-order accuracy in space for steady case [20]. The results of this calculation are carried out using a grid space of $\Delta x = 2.5\,\mathrm{m}$ grid. The proposed model located the sharp discontinuities of the corresponding stationary solution. Thus, this model also could efficiently deal with multiple hydraulic jumps for steady flow over a ladder of weirs.

6. CONCLUSIONS

In the present work, we reformulated a version of the RKDG2 with a simple way to incorporate source terms and a robust procedure to cope with boundary conditions. The performance of the

DOI: 10.1002/fld

overall technique was shown in several examples going from the standard dam-break problem to a selection of discontinuous steady flow tests, as well as to compute flow over compound branches coupled with internal boundary conditions.

For a better evaluation, a widely used traditional TVD-FV2 method has been considered and implemented invoking: the same Riemann solver; the same slope limiter; the same boundary conditions treatment; and the same manner of discretizing source terms. In all the investigated problems, the RKDG2's results were depicted together with the FV2's results all to be weighted against an available reference solution. Strong numerical evidence shows the ability of the RKDG2 scheme to provide accurate solutions in proper agreement with the reference solution. Hence, it can be concluded that the discussed scheme is accurate, straightforward, efficient and robust and can be of practical consideration when solving shallow water flows involving: non-prismatic channels; various cross-sections; smooth topology variation; and internal boundary conditions.

However, even though the simple treatment the source terms has achieved promising results when employed within the RKDG2 method, unfortunately, it was unable to cope with problems involving discontinuous bed topography. Hence, future work will consist of applying a more robust procedure of treating the source vector with the RKDG2 method.

REFERENCES

1. García-Navarro P, Alcrudo F, Savirón JM. 1-D open channel flow simulation using TVD McCormack scheme. *Journal of Hydraulic Engineering* 1992; **118**(10):1359–1372.
2. Hirsch C. *Computational Methods for Inviscid and Viscous Flows*: *Numerical Computation of Internal and External Flows*. Wiley: New York, 1990.
3. Bermudez A, Vázquez ME. Upwind methods for hyperbolic conservation laws with source terms. *Computer and Fluids* 1994; **23**(8):1049–1071.
4. Vázquez-Cendón ME. Improved treatment of source terms in upwind schemes for the shallow water equations in channels with irregular geometry. *Journal of Computational Physics* 1999; **148**(2):497–526.
5. Hubbard ME, García-Navarro P. Flux difference splitting and the balancing of source terms and flux gradients. *Journal of Computational Physics* 2000; **165**(1):89–125.
6. Zhou JG, Causon DM, Mingham CG, Ingram DM. The surface gradient method for the treatment of source terms in the shallow-water equations. *Journal of Computational Physics* 2001; **168**(1):1–25.
7. Cockburn B, Shu CW. Foreword (for the special issue on discontinuous Galerkin methods). *Journal of Scientific Computing* 2005; **22–23**:1–2.
8. Cockburn B, Shu CW. Runge–Kutta discontinuous Galerkin method for convection-dominated problems. *Journal of Scientific Computing* 2001; **16**(3):173–261.
9. Cockburn B. Discontinuous Galerkin methods. *ZAMM* 2003; **83**(11):731–754.
10. Schwanenberg D, Kongeter J. A discontinuous Galerkin method for the shallow water equations with source terms. In *Discontinuous Galerkin Methods*, Cockburn B, Karniadakis G, Shu CW (eds). Lecture Notes in Computational Science and Engineering, vol. 11. Springer: Berlin, 2000; 419–424.
11. Roe PL. Approximate Riemann solvers, parameter vectors, and difference schemes. *Journal of Computational Physics* 1981; **43**(2):357–372.
12. Shu C-W, Osher S. Efficient implementation of essentially non-oscillatory shock capturing schemes. *Journal of Computational Physics* 1988; **77**(2):439–471.
13. Osher S. Convergence of generalized MUSCL schemes. *SIAM Journal on Numerical Analysis* 1984; **22**(5): 947–961.
14. Sweby PK. High resolution schemes using flux limiters for hyperbolic conservation laws. *SIAM Journal on Numerical Analysis* 1984; **21**(5):995–1011.
15. Van Leer B. Towards the ultimate conservation difference scheme, V. *Journal of Computational Physics* 1979; **32**(1):101–136.
16. Harten A, Lax PD, van Leer B. On upstream differencing and Godunov-type schemes for hyperbolic conservation laws. *SIAM Review* 1983; **25**(1):35–61.

DOI: 10.1002/fld

17. Xing Y, Shu CW. A new approach of high order well-balanced finite volume WENO schemes and discontinuous Galerkin methods for a class of hyperbolic systems with source terms. *Communication in Computational Physics* 2006; **1**(1):100–134.
18. García-Navarro P, Savirón JM. McCormack's method for the numerical simulation of one-dimensional discontinuous unsteady open channel flow. *Journal of Hydraulic Research* 1992; **30**(1):95–105.
19. Alcrudo F, Benkhaldoun F. Exact solutions to the Riemann problem of the shallow water equations with a bottom step. *Computers and Fluids* 2001; **30**(6):643–671.
20. Burguete J, García-Navarro P. Improving simple explicit methods for unsteady open channel and river flow. *International Journal for Numerical Methods in Fluids* 2001; **45**(2):125–156.
21. McDonald I. Analysis and computation of steady open channel flow. *Ph.D. Thesis*, University of Reading, 1996.
22. Chow VT. *Open-channel Hydraulics*. McGraw-Hill: New York, 1959.
23. García-Navarro P, Vázquez-Cendón ME. On numerical treatment of the source terms in shallow water equations. *Computers and Fluids* 2000; **29**(8):951–979.
24. Courant R, Friedrichs KO, Lewy H. Über die partiellen differenzangleichungen der mathematisches. *Mathematische Annalen* 1928; **100**(1):32–74.

DOI: 10.1002/fld